Atmos. Chem. Phys. Discuss., 12, 14363–14392, 2012
www.atmos-chem-phys-discuss.net/12/14363/2012/
doi:10.5194/acpd-12-14363-2012

Atmospheric Chemistry and Physics Discussions

Estimation of lifetime of carbonaceous aerosol from open crop residue burning during Mount Tai Experiment 2006 (MTX2006)

X. L. Pan[1,2], Y. Kanaya[1], Z. F. Wang[2], Y. Komazaki[1], F. Taketani[1], H. Akimoto[3], P. Pochanart[4], and Y. Liu[2]

[1]Research Institute for Global Change, Japan Agency for Marine-Earth Science and Technology, Japan
[2]State Key Laboratory of Atmospheric Boundary Layer Physics and Atmospheric Chemistry, Institutes of Atmospheric Physics, Chinese Academy of Sciences, Beijing, China
[3]Acid Depositions and Oxidant Research Center, Asia Center for Air Pollution Research, Japan
[4]School of Social and Environmental Development, National Institute of Development Administration, Bangkok, Thailand

Received: 1 May 2012 – Accepted: 12 May 2012 – Published: 7 June 2012

Correspondence to: X. L. Pan (xlpanelf@gmail.com)

Published by Copernicus Publications on behalf of the European Geosciences Union.

ACPD

12, 14363–14392, 2012

Abstract

Studying the emission ratios of carbonaceous aerosols (element carbon, EC, and organic carbon, OC) from open biomass burning helps to reduce uncertainties in emission inventories and provides necessary constraints for model simulations. We measured apparent elemental carbon (EC_a) and OC concentrations at the summit of Mount Tai (Mt. Tai) during intensive open crop residue burning (OCRB) episodes using a Sunset OCEC analyzer. Equivalent black carbon (BC_e) concentrations were determined using a Multiple Angle Absorption Photometer (MAAP). In the fine particle mode, OC and EC showed strong correlations ($r > 0.9$) with carbon monoxide (CO). Footprint analysis using the FLEXPART_WRF model indicated that OCRB in central east China (CEC) had a significant influence on ambient carbonaceous aerosol loadings at the summit of Mt. Tai. $\Delta EC_a/\Delta CO$ ratios resulting from OCRB plumes were $14.3 \pm 1.0\,ng\,m^{-3}\,ppbv^{-1}$ at Mt. Tai. This ratio was more than three times those resulting from urban pollution in CEC, demonstrating that significant concentrations of soot particles were released from OCRB. $\Delta OC/\Delta CO$ ratio from fresh OCRB plumes was found to be $41.9 \pm 2.6\,ng\,m^{-3}\,ppbv^{-1}$ in PM_1. The transport time of smoke particles was estimated using the FLEXPART_WRF tracer model by releasing inert particles from the ground layer inside geographical regions where large numbers of hotspots were detected by a MODIS satellite sensor. Fitting regressions using the e-folding exponential function indicated that the removal efficiency of OC (normalized to CO) was much larger than that of EC_a mass, with mean lifetimes of 27 h (1.1 days) for OC and 105 h (4.3 days) for EC_a, respectively. The lifetime of black carbon estimated for the OCRB events in east China was comparably lower than the values normally adopted in the transport models. Short lifetime of organic carbon highlighted the vulnerability of OC to cloud scavenging in the presence of water-soluble organic species from biomass combustion.

ACPD
12, 14363–14392, 2012

1 Introduction

Open biomass burning (OBB, including disposal of crop residues and wild fires in grassland/forest areas) has significant impacts on regional air quality (Crounse et al., 2009), including increased atmospheric turbidity (Badarinath et al., 2004), tropospheric ozone variability (Kondo et al., 2004) and respiratory disease morbidity (Arbex et al., 2007). Carbonaceous aerosol particles (such as black carbon (BC) and organic carbon (OC)) released from burning can be incorporated into cloud processes, eventually influencing regional climate changes (Jourdain et al., 2007; Tosca et al., 2010). Intensive open crop residue burning (OCRB) during the harvest season in east China has recently become a significant concern. It has been reported that approximately 30–80 % of agricultural residues were used as biomass fuels, and that approximately one third of crop biomass was openly combusted in fields (Yamaji et al., 2010). In studies of Asian regional pollution transport and ozone photochemistry, discrepancies between observations and model simulations were partly attributed to biases in estimated open biomass burning emissions (uncertainties > 450 % at the 95 % confidence interval) (Streets et al., 2003).

Emissions characteristics of trace gases and aerosol particles from biomass burning have been compiled in the literature (Andreae and Merlet, 2001). For corroboration, emission ratios of aerosols to carbon monoxide obtained from in-situ observations and laboratory experiments could serve as excellent constraints for improving their emission inventories. Previous studies indicated that emission ratios of black carbon to CO from OBB were $25\,\mathrm{ng\,m^{-3}\,ppbv^{-1}}$ in India (Badarinath et al., 2007), $2.3 \pm 2.2\,\mathrm{ng\,m^{-3}\,ppbv^{-1}}$ in North America (Kondo et al., 2011) and $\sim 11\,\mu\mathrm{g\,m^{3}\,ppbv^{-1}}$ in eastern China (Pan et al., 2011). Differences among biofuel types, combustion phases, diffusion conditions and dry deposition processes likely resulted in the large variations measured (Andreae and Merlet, 2001). Freshly produced soot particles are theoretically graphite homologues and are hydrophobic, tending to preserve their characteristics during long-distance transport. Measured OC emission ratio, however, vary widely

ACPD
12, 14363–14392, 2012

among studies due to different emission scenarios, condensation or formation of secondary organic species and removal processes (Maria et al., 2003). Better estimation of its lifetime, especially for BC, is crucial for regional/global transport model. Investigations on basis of theoretical BC modules have been performed for decade, and different hypotheses of mixing state, size distribution and hydrophilic properties of BC could lead to significant varieties in the lifetime, ranging from 4.7 to 98 days (Croft et al., 2005; Stier et al., 2005). In quantifying climate effect of BC, employing different aging parameters from region to region was much reasonable than using a global unique value. Unfortunately investigation of lifetime of BC from perspective of field measurements was still limited, especially in the East Asia region. In the present study, we examined variations in the carbonaceous aerosol correlations of smoke particles observed at the summit of Mount Tai (Mt. Tai) in Central East China (CEC) during the harvest season, in relation to the transport time from the burned area. It should be noted that soot particles in this study were determined using a Sunset Laboratory semi-continuous OCEC analyzer and the term "apparent elemental carbon" (EC_a, operationally defined as the fraction of refractory carbon compounds in the presence of oxygen) was adopted in this context because of uncertainties arising from artificial temperature control protocols (Andreae and Gelencser, 2006). Black carbon mass was determined using optical techniques and was defined as "equivalent black carbon" (BC_e).

2 Experimental

Carbonaceous aerosol concentration measurements were performed on the summit of Mt. Tai (36.26° N, 117.11° E, 1534 m a.s.l.) during a field campaign termed MTX2006 (Fig. 1). Mt. Tai is an isolated peak in the middle of central east China (CEC) where open biomass burning in the surrounding areas was active during the harvest season (June). Carbonaceous aerosol emissions from biomass burning and their impact on the regional environment have been reported (Fu et al., 2008; Li et al., 2008; Inomata et al., 2009; Yamaji et al., 2010). Concentrations of EC_a and OC were determined using

ACPD
12, 14363–14392, 2012

an OCEC analyzer (Sunset Lab) equipped with a PM_1 cyclone (1 µm diameter cutoff, URG-2000-30EHB, URG Inc.) with a time resolution of 1 h. The NIOSH temperature protocol (600 °C (holding 80 s), 840 °C (holding 90 s), oven off (holding 55 s) in pure He; afterward 550 °C (holding 30 s), 850 °C (holding 110 s) and oven off (85 s) in an O_2/He environment) was used from 2 June, 13:00 LST to 20 June, 04:00 LST. Calibration using standard CH_4 gas was performed for 120 s at the end of each analysis. Comparisons between EC_a measurements using the IMPROVE and NIOSH protocols at Mt. Tai suggested a systematic bias of 31 %. Uncertainties in OC measurements were less than ±25 %. A detailed description of instrumentation and temperature program used has previously been reported (Kanaya et al., 2008). BC_e mass was measured using a multiple angle absorption photometer (MAAP5012, Thermo) whose uncertainty was estimated to be less than 15 %. A fixed mass-specific aerosol absorption coefficient (MAC) of 6.6 $m^2\,g^{-1}$ at a wavelength (λ) of 637 nm was adopted to convert the absorption coefficient to mass concentrations. Sampling was alternated between PM_1 and $PM_{2.5}$ using an automated valve switch between two cyclones (URG-2000-30EHB and URG-2000-30EH, URG Inc.) every 30 min.

CO mixing ratios were measured using a gas filter non-dispersive infrared carbon monoxide gas analyzer (Thermo Electron Co., Model 48C). Zero calibrations were performed during the first 10 min of each hour using purified air (Thermo Electron Co., Model 111). Span calibrations were performed using a standard CO gas (1.59 ppmv, produced by Taiyo Nissan Corp., Japan). Uncertainties were less than 5 %.

3 Results and discussion

3.1 Identification of OCRB episodes and supporting observations

At Mt. Tai, OCRB-dominated pollution episodes were determined from measurements of biomass burning tracers. Two discrete OCRB plumes (6 June, 00:00–7 June, 09:00 LST and 12 June, 00:00–13 June, 12:00 LST) were identified based on highly

ACPD
12, 14363–14392, 2012

elevated concentrations of levoglucosan (459 ng m^{-3}) and galactosan (12.8 ng m^{-3}), measured using GC-MS (Fu et al., 2008). High ΔNMVOCs/ΔCO ratios (acetonitrile, formaldehyde, acetaldehyde, etc.) were also reported by Inomata et al. (2010) using PTR-MS during OCRB pollution episodes. Smoke tracer such as CH_3Cl and CH_3Br also have been reported to have higher $\Delta CH_3Cl/\Delta CO$ and $\Delta CH_3Br/\Delta CO$ ratios during OCRB episodes, with mean values of 1.88 (r = 0.82) and 0.012 (r = 0.72), respectively (Suthawaree et al., 2010). OCRB emissions accounted for 26 %, 62 %, 79 % and 80 % of O_3, CO, BC and OC concentrations, respectively, at the summit of Mt. Tai based on simulations using the models-3 community multi-scale air quality modeling system (CMAQ) (Yamaji et al., 2010).

In this study, footprint regions (<100 m height) for the air masses sampled at Mt. Tai were determined using the FLEXPART_WRF model (Version 6.2), running in a backward mode, simulating the transport of 30000 tracer particles released from the measurement site. Detailed specifications of the FLEXPART model have been reported (Stohl et al., 1998). The 3D-meteorological field was calculated using WRF (Version 3.3) with spatial resolution of 75 km × 75 km. The initial input meteorological NCEP/FNL data were obtained from the Global Data Assimilation System (GDAS, http://dss.ucar.edu/datasets/ds083.2/). As shown in Fig. 2c and d, the footprint regions covered nearly all the hotspots detected by the Aqua/Terra MODIS satellite, providing evidence of the potential influence from ground-based OCRB emissions.

3.2 Carbonaceous aerosol mass loadings

Time-series of carbonaceous aerosol measurements at Mt. Tai are presented in Fig. 3. It was noted that during OCRB-dominated episodes EC_a concentrations peaked twice (7 June, 06:00 LST and 13 June, 04:00 LST), with hourly mean values of 18.9 and 22.4 μg m^{-3}, respectively. The corresponding OC concentrations were 58.9 and 76.7 μg m^{-3}, respectively. From 8 June–11 June, ambient carbonaceous aerosol concentrations were low because the air masses were largely transported from the

ACPD
12, 14363–14392, 2012

Mongolian Plateau region and the impacts from ground emissions on these air masses were weak. Concentrations of CO, CO_2 and BC_e showed similar temporal variations. At the summit of Mt. Tai, mean EC_a and OC concentrations during OCRB episodes were 7.3 and 30.1 $\mu g\,m^{-3}$, respectively, 5–6 times higher than those (EC_a: 1.6 $\mu g\,m^{-3}$ and OC: 5.3 $\mu g\,m^{-3}$) during non-OCRB episodes. BC_e concentrations in PM_1 and $PM_{2.5}$ were alternately measured using an automated switching valve. Good consistencies between $PM_1$and $PM_{2.5}$ were observed during OCRB-dominant and non-OCRB periods (Fig. 4). Linear regression fitting indicated that the $BC_e(PM_{2.5})/BC_e(PM_1)$ ratio was 1.05 (r = 0.88) during OCRB episodes, slightly higher than that (1.02, r = 0.96) for non-OCRB episodes, suggesting that mass concentration of EC_a in PM_1 contributed to over 95 % EC_a mass in $PM_{2.5}$. This result is consistent with past studies suggesting that the volume equivalent median diameters of smoke particles ranged from 100 to 300 nm (Reid et al., 2005; Schwarz et al., 2008; Hosseini et al., 2010).

3.3 Carbonaceous aerosol correlations

Carbonaceous aerosol relationships during OCRB episodes were characterized using linear regressions of concentrations of the species of interest versus the reference gas, described as $\Delta(x)/\Delta CO = ((x)_{ORCB}\text{-}(x)_{baseline})/(CO_{ORCB}\text{-}CO_{baseline})$. CO was selected as the reference gas because of its incomplete combustion origins and relatively long lifetime in the atmosphere. In this study, x represented EC_a and OC (in $ng\,m^{-3}$). The impact of CO production from the oxidation of volatile organic compounds (VOCs) was assumed to be weak because the concentrations of VOCs during OCRB episodes were smaller than the ambient CO loadings in CEC and because the oxidation rates of the VOCs were insufficient considering that the OCRB episodes occurred at night and that the typical transport time from the source region was <40 h (see Sect. 3.4).

ACPD
12, 14363–14392, 2012

3.3.1 $\Delta EC_a/\Delta CO$ ratios

Strong EC_a-CO correlations were found during the identified OCRB episodes. Overall, the average $\Delta EC_a/\Delta CO$ ratios in OCRB plume was 14.3 ng m^{-3} ppbv^{-1} at Mt. Tai (Fig. 5). Detailed descriptions of mass concentrations of carbonaceous aerosols and its correlations are listed in Table 2. The values measured at Mt. Tai were comparable with airborne measurements made using a single particle soot photometer (SP2) during the 2006 TexAQS campaign (average $\Delta BC/\Delta CO$ of 13.8 ng m^{-3} ppbv^{-1}, converted from a $\Delta CO/\Delta CO_2$ ratio of 102 ± 25 ppbv ppmv^{-1} and a $\Delta BC/\Delta CO_2$ ratio of 1770 ± 400 ng BC kg^{-1} air ppmv^{-1}) in fresh OBB plumes. The ratios in this study were approximately 50 % higher than those reported by Andreae and Merlet (2001) ($\Delta EC_a/\Delta CO$ ratios of 9.4 ng m^{-3} ppbv^{-1} for agricultural residue burning, converted from units of g(EC)/g(CO), assuming a molar volume of 22.4 L under STP conditions for CO) and measurements (10.3–11.6 ng m^{-3} ppbv^{-1} for open biomass burning plumes) at Mt. Huang in eastern China (Pan et al., 2011). The $\Delta EC_a/\Delta CO$ ratio at Mt. Tai was similar to those reported for emissions from residential wood burning stoves commonly used in some rural communities (Roden et al., 2006; Shen et al., 2010). This result was reasonable because OCRB was normally characterized by fixed-size biomass piles with early intense flaming combustion and later smoldering combustion with lower temperature that produce larger condensation nuclei and un-combusted condensate (Reid et al., 1998, 2005). It is worthy to note that aerosol particles from OCRB sampled at the summit of Mt. Tai generally had transport times of more than 10 h after being released. The average relative humidity of the air mass over the 3-day back-trajectories was found to be ~50 % based on ensemble calculations using the Hysplit model (version 4.9), which indicating that aging processes and consequent cloud scavenging likely affected.

3.3.2 $\Delta OC/\Delta CO$ ratios

Previous studies have demonstrated that the carbon/oxygen content of biofuels, combustion phase, atmospheric photochemistry and removal processes can lead to large

ACPD
12, 14363–14392, 2012

variations in observed ΔOC/ΔCO ratios for biomass burning plumes. At the summit of Mt. Tai, apparent increases in ΔOC/ΔCO ratios were observed during OCRB episodes (Fig. 5). The average ΔOC/ΔCO ratio was found to be $41.9 \pm 2.6\,ng\,m^{-3}\,ppbv^{-1}$, similar with that ($44.8\,ng\,m^{-3}\,ppbv^{-1}$) reported by Andreae and Merlet (2001) for the burning of agricultural residues. However, our result was lower than the values for pine-savanna fires ranging from 70.5 to $105.8\,ng\,m^{-3}\,ppbv^{-1}$ (Yokelson et al., 2007), derived from ΔOA(organic aerosols)/ΔCO ratio of $148\,ng\,m^{-3}\,ppbv^{-1}$ assuming ΔOA/ΔOC = 1.4–2.1, and aircraft measurement of the ΔOA/ΔCO ratio ($165\,ng\,m^{-3}\,ppbv^{-1}$) for OBB during the MILAGRO campaign (DeCarlo et al., 2010), assuming the similar ΔOA/ΔOC range. Measurements in Guangzhou demonstrated that the mass size distribution of OC had a peak diameter between 1–1.8 µm in biomass burning smoke (Yu, 2009). At Mt. Tai, OC concentrations were measured using a cutoff of PM_1 and the exclusion of OC with aerodynamic diameters larger than 1 µm might have led to an underestimation of the ambient ΔOC/ΔCO ratio. However, airborne sampling of biomass burning plumes in North America (Clarke et al., 2007) found that the submicron fraction of OC may also be substantial, and Δvolatile OC (fraction of OC lost by heating to 400°C)/ΔCO and Δ refractory OC (fraction of OC not lost by heating to 400°C)/ΔCO ratios were 91 ± 3 and $34 \pm 3\,ng\,m^{-3}\,ppbv^{-1}$, respectively, much higher than the observation at summit of Mt. Tai. The preferential loss of OC during its upward transport could provide a plausible explanation for this. In the next section, we study the features as time evolution of the ΔOC/ΔCO ratio, using the transport time.

3.4 Impact of transport on carbonaceous aerosol relationships

3.4.1 Definition of transport time

The transport times of smoke particles sampled at each site were calculated based on forward simulations using the FLEXPART-WRF model by releasing specific numbers of tracer particles (N = 30 000) from areas where OCRB occurred. In principle, it was impossible to determine the exact occurrence times, durations and geographic locations

ACPD
12, 14363–14392, 2012

of OCRB episodes in the CEC. We estimated the locations of OCRB activities according to hotspot data derived from MODIS satellite remote sensing. Tracer particles were released from identified geographical regions (latitude 33° N–34° N; longitude 116° E–118° E) at heights between 5–10 m from 4 June, 18:00 LST–18 June, 23:00 LST at a fixed time interval (1 h). As shown in Fig. 2a and b, the upward transport pattern of OCRB plumes was excellently captured by the model. The transport time (T) of a single smoke particle (i), released at local time (t_0) and sampled at local time (t) was expressed as:

$$T_{\text{transport time }(i)} = T(i) - T_0(i) \quad (1)$$

The characteristic transport time of a set of particles (N) sampled at the site at time $t$was defined as its arithmetic average:

$$\bar{T} = \frac{1}{N}\sum_{i=1}^{N} T_{(i)} \quad (2)$$

Uncertainties were estimated as their standard deviations:

$$\sigma = \sqrt{\frac{1}{N-1}\sum_{i=1}^{N}(T_i - T)^2} \quad (3)$$

In the Mt. Tai campaign, we calculated the $\Delta EC_a/\Delta CO$, $\Delta OC/\Delta CO$ and $\Delta OC/\Delta EC_a$ ratios over a time window of 6 h and moved the analysis time window from 6 June, 10:00 to 7 June, 09:00 LST and from 12 June, 18:00 to 13 June, 09:00 LST at a time step of 3 h. The corresponding transport times of tracer particles sampled at the site were estimated according to Eqs. (2) and (3). Sensitivity tests with different time windows (ranging from 5 to 7 h) only caused ~10 % variation in $\Delta EC_a/\Delta CO$ ratios and less than 5 % variations in $\Delta OC/\Delta CO$ and $\Delta OC/\Delta EC_a$ ratios.

ACPD
12, 14363–14392, 2012

3.4.2 Estimated loss rate of EC_a and OC

The relationship between carbonaceous aerosol ratios and transport time at Mt. Tai is presented in Fig. 6. Generally, we found that the $\Delta EC_a/\Delta CO$, $\Delta OC/\Delta CO$ and $\Delta OC/\Delta EC_a$ ratios declined with increasing transport time from T< 1 h to T> 40 h. For clarification, we classified the transport time into three subgroups (T< 15 h, 20 <T30 h and > 30 h). As shown in Table 3, $\Delta EC_a/\Delta CO$ ratios decreased from 14.5 to 10.5 $\mu g\,m^3\,ppbv^{-1}$ when the transport time increased from 10 h to 32.7 h (~40 % decrease). Our recent field measurement at Rudong (in East China, on June 2010) indicated that smoke particles had $\Delta EC_a/\Delta CO$, $\Delta OC/\Delta CO$ ratios of 15.5 $ng\,m^{-3}\,ppbv^{-1}$ and 97.7 $ng\,m^{-3}\,ppbv^{-1}$ respectively when observation was in the proximity of OCRB sources (Pan et al., 2012). The age of smoke particles (~0.7 h) from OCRB were only roughly determined by dividing the maximum geographic distance (10 km) by the local wind speed, since FLEXPART-WRF model was unable to estimate the exact age of tracer particles sampled due to the coarse spatial resolution (75 km × 75 km) of the simulations. Herein the results at Rudong (only one point, the filled-triangle in Fig. 6) were also included in the following curve fitting regressions. The fitting equation is as following:

$$f(x) = A \times \exp(-1 \cdot \frac{x}{\tau}), \quad (4)$$

Where the independent variable x corresponds to transport time and τ indicates the lifetime of carbonaceous aerosols. Relationships between $\Delta EC_a/\Delta CO$ ratios and OCRB smoke transport time are presented in Fig. 6a. The fitting curve suggested that the emission ratio of EC_a from OCRB under the initial conditions (y-intercept of fitting curve) was 15.9 $ng\,m^{-3}\,ppbv^{-1}$. The lifetime of EC_a was determined to be 105 h (4.3 days) with extreme large uncertainty (seen the gray line in Fig. 6a). Fitting result only with the data (correlations efficient greater than 0.95) indicated that ECa lifetime was 106 h (4.4 days) with standard deviation (σ: ± 3.5 days). The black carbon lifetime has

ACPD
12, 14363–14392, 2012

been estimated in the past model-based studies (Table 4). Our value is lower than estimations (6–10 days) derived from simulations of the global black carbon model (Cooke and Wilson, 1996). Simulations of the TRACE-P period using the GEOS-chem model indicated that black carbon outflowing from East Asia had a lifetime of 5.8 ± 1.8 days (Park et al., 2005), comparable to our results. A sensitivity test with an off-line global transport chemistry model (TM5) indicated that lifetime of BC was 4.7 days under the presumption that BC was externally mixed in the accumulation mode and did not experience any changes in the hygroscopic properties due to aging; however, a longer BC lifetime (6.2 days) was expected if aging processes (condensation of H_2SO_4 and coagulation with soluble particles) and size distribution of BC masses were taken into considerations (Vignati et al., 2010). Furthermore, Croft et al. (2005) suggested that the BC lifetime can vary with the processes (condensation, coagulation, and oxidation) we take into account, suggesting that better understanding of chemical processes in different atmospheric environment is essential, rather than estimating a single lifetime of BC over a global scale. In the present study we have just reported the overall lifetime of OCRB-derived black carbon without specifying the explicit processes involved. Additional uncertainty might be introduced from systematic bias inherent to the measurement method. However we found very similar estimations by using $\Delta EC_a/\Delta CO_2$, $\Delta BC_e/\Delta CO$ and $\Delta BC_e/\Delta CO_2$ ratios with means of 113 h (4.7 days), 116 h (4.8 days) and 104 h (4.3 days), and thus the additional uncertainty is not large.

Regression fitting (Fig. 6b) illustrated that OC from OCRB had a much faster loss rate than that of EC_a. The net lifetime of OC in OCRB smoke was estimated to be 27 h (1.1 days). Based on filter-based sampling, ~64 % of OC in $PM_{2.5}$ from OCRB smoke was identified to be water-soluble (Fu et al., 2008), suggesting that OC is susceptible to cloud scavenging processes. Field studies of OBB smoke in the Yucatan indicated rapid secondary organic aerosol formation could lead to OA/CO ratios more than doubling in 1.4 ± 0.7 h (Yokelson et al., 2007). Conceptual models have also demonstrated that $\Delta OA/\Delta CO$ ratios can double within photochemical ages of less than 50 h because of oxidation and the formation of less volatile organics (Dunlea et al., 2009) while the

ACPD
12, 14363–14392, 2012

ratio can also decrease dramatically from scavenging processes of organics. Here we should note the difference between OC and OA; as opposed to OC, OA can be increased by the acquisition of oxygen atoms in the particles. Therefore the OC might be influenced more strongly by the loss. In the present study we did observe a gradual decreasing trend. The y-intercept from linear fitting was found to be 80.3 ng m^{-3} $ppbv^{-1}$; approximately 20 % lower than the ΔOC/ΔCO ratio measured in the fresh plumes during the Rudong campaign mentioned earlier.

The $\Delta OC/\Delta EC_a$ ratios also decreased with increasing transport time (Fig. 6c). According to fitting results, the $\Delta OC/\Delta EC_a$ ratio for fresh smoke in the submicron mode was 7.7 (y-intercept) and the $\Delta OC/\Delta EC_a$ ratio in $PM_{2.5}$ was estimated to be 12.8, assuming that the OC mass in PM_1 accounted for 60 % of the OC mass in $PM_{2.5}$ (Yu, 2009). Our result was 64 % higher than the values reported by Andreae and Merlet (2001) (4.7) and airborne measurements (OC/EC_a = 6.25) in southern Africa during the dry biomass burning season (Kirchstetter et al., 2003). In India, the $\Delta OC/\Delta EC_a$ ratios of indoor biomass burning (Rehman et al., 2011) and outdoor wood-fuel/agricultural waste burning (Ram and Sarin, 2010) were reported to be 5.3 ± 1.6 and 7.8 ± 2.4, respectively, considerably less than the value in this study. These differences could result from the variety of biomass burned and different combustion conditions. During OCRB episodes in CEC, crop residues to be burnt were normally piled up or bundled together. These conditions easily produce oxygen-limited conditions in the interior flaming zone and lower external temperatures during the later smoldering stages, which tends to produce more organic particles because of the condensation of volatilized matter on any available nuclei or un-combusted condensate (Reid et al., 2005).

4 Conclusions

In the present study, we analyzed ambient concentrations of carbonaceous aerosols (including EC_a, OC, BC_e, CO, CO_2) measured during the intensive OCRB season at the summit of Mt. Tai in central east China. Concentrations of EC_a and OC were

ACPD
12, 14363–14392, 2012

determined using a Sunset OCEC analyzer with the NIOSH temperature control protocol and BC_e concentrations were determined using a multiple angle absorption photometer. The impact of OCRB on ambient carbonaceous aerosol correlations was determined using $\Delta EC_a/\Delta CO$ and $\Delta OC/\Delta CO$ ratios. As expected, strong positive correlations between ambient EC_a and OC masses and CO mixing ratios were observed during OCRB-dominant episodes. The average $\Delta EC_a/\Delta CO$ and $\Delta OC/\Delta CO$ ratios were $14.3 \pm 1.0\,ng\,m^{-3}\,ppbv^{-1}$ and $41.9 \pm 2.6\,ng\,m^{-3}\,ppbv^{-1}$, respectively. Based on forward simulations using the FLEXPART_WRF tracer model, we estimated the transport time of smoke particles by releasing specific numbers of inert particles from areas where OCRB occurred according to geographical hotspot distributions observed by a MODIS satellite sensor. The dependences of $\Delta EC_a/\Delta CO$ and $\Delta OC/\Delta CO$ ratios on transport time were also presented. An e-folding equation fitting demonstrated that EC_a (normalized to CO) had a mean lifetime of ~4.3 days. The lifetime of OC estimated in the same way was shorter, 1.1 days, suggesting a faster net loss process of OC including cloud scavenging. The lifetime of black carbon estimated by means of different carbonaceous aerosol correlation ($\Delta EC_a/\Delta CO_2$, $\Delta BC_e/\Delta CO$ and $\Delta BC_e/\Delta CO_2$) was similar (4.2–4.8 days). Our study suggested that it was necessary to use the regional-specific aging parameters of carbonaceous aerosols when studying the transport of biomass burning plumes.

Acknowledgements. The authors would like to thank Hiroshi Tanimoto (National Institute of Environmental Studies) and Yele Sun (State Key Laboratory of Atmospheric Boundary Layer Physics and Atmospheric Chemistry, Institute of Atmospheric Physics) for valuable comments. We gratefully acknowledge the anonymous reviewers for their helpful comments and suggestions. This work was supported by the Global Environment Research Fund (S-7, C-081, B-051) from the Ministry of the Environment, Japan.

ACPD
12, 14363–14392, 2012

References

Andreae, M. O. and Gelencsér, A.: Black carbon or brown carbon? The nature of light-absorbing carbonaceous aerosols, Atmos. Chem. Phys., 6, 3131–3148, doi:10.5194/acp-6-3131-2006, 2006.

Andreae, M. O. and Merlet, P.: Emission of trace gases and aerosols from biomass burning, Global Biogeochem Cy., 15, 955–966, 2001.

Arbex, M. A., Martins, L. C., de Oliveira, R. C., Pereira, L. A. A., Arbex, F. F., Cançado, J. E. D., Saldiva, P. H. N., and Braga, A. L. F.: Air pollution from biomass burning and asthma hospital admissions in a sugar cane plantation area in Brazil, J. Epidemiol. Commun. H., 61, 395–400, doi:10.1136/jech.2005.044743, 2007.

Badarinath, K. V. S., Madhavi Latha, K., Kiran Chand, T. R., Gupta, P. K., Ghosh, A. B., Jain, S. L., Gera, B. S., Singh, R., Sarkar, A. K., Singh, N., Parmar, R. S., Koul, S., Kohli, R., Nath, S., Ojha, V. K., and Singh, G.: Characterization of aerosols from biomass burning – a case study from Mizoram (Northeast), India, Chemosphere, 54, 167–175, doi:10.1016/j.chemosphere.2003.08.032, 2004.

Badarinath, K. V. S., Kharol, S. K., Chand, T. R. K., Parvathi, Y. G., Anasuya, T., and Jyothsna, A. N.: Variations in black carbon aerosol, carbon monoxide and ozone over an urban area of Hyderabad, India, during the forest fire season, Atmos. Res., 85, 18–26, 2007.

Clarke, A., McNaughton, C., Kapustin, V., Shinozuka, Y., Howell, S., Dibb, J., Zhou, J., Anderson, B., Brekhovskikh, V., and Turner, H.: Biomass burning and pollution aerosol over North America: Organic components and their influence on spectral optical properties and humidification response, J. Geophys. Res, 112, D12S18, doi:10.1029/2006JD007777, 2007.

Cooke, W. F. and Wilson, J. J. N.: A global black carbon aerosol model, J. Geophys. Res.-Atmos., 101, 19395–19409, 1996.

Croft, B., Lohmann, U., and von Salzen, K.: Black carbon ageing in the Canadian Centre for Climate modelling and analysis atmospheric general circulation model, Atmos. Chem. Phys., 5, 1931–1949, doi:10.5194/acp-5-1931-2005, 2005.

Crounse, J. D., DeCarlo, P. F., Blake, D. R., Emmons, L. K., Campos, T. L., Apel, E. C., Clarke, A. D., Weinheimer, A. J., McCabe, D. C., Yokelson, R. J., Jimenez, J. L., and Wennberg, P. O.: Biomass burning and urban air pollution over the Central Mexican Plateau, Atmos. Chem. Phys., 9, 4929–4944, doi:10.5194/acp-9-4929-2009, 2009.

ACPD
12, 14363–14392, 2012

DeCarlo, P. F., Ulbrich, I. M., Crounse, J., de Foy, B., Dunlea, E. J., Aiken, A. C., Knapp, D., Weinheimer, A. J., Campos, T., Wennberg, P. O., and Jimenez, J. L.: Investigation of the sources and processing of organic aerosol over the Central Mexican Plateau from aircraft measurements during MILAGRO, Atmos. Chem. Phys., 10, 5257–5280, doi:10.5194/acp-10-5257-2010, 2010.

Dunlea, E. J., DeCarlo, P. F., Aiken, A. C., Kimmel, J. R., Peltier, R. E., Weber, R. J., Tomlinson, J., Collins, D. R., Shinozuka, Y., McNaughton, C. S., Howell, S. G., Clarke, A. D., Emmons, L. K., Apel, E. C., Pfister, G. G., van Donkelaar, A., Martin, R. V., Millet, D. B., Heald, C. L., and Jimenez, J. L.: Evolution of Asian aerosols during transpacific transport in INTEX-B, Atmos. Chem. Phys., 9, 7257–7287, doi:10.5194/acp-9-7257-2009, 2009.

Fu, P., Kawamura, K., Okuzawa, K., Aggarwal, S. G., Wang, G., Kanaya, Y., and Wang, Z.: Organic molecular compositions and temporal variations of summertime mountain aerosols over Mt. Tai, North China Plain, J. Geophys. Res, 113, D19107, doi:10.1029/2008JD009900, 2008.

Inomata, S., Tanimoto, H., Kato, S., Suthawaree, J., Kanaya, Y., Pochanart, P., Liu, Y., and Wang, Z.: PTR-MS measurements of non-methane volatile organic compounds during an intensive field campaign at the summit of Mount Tai, China, in June 2006, Atmos. Chem. Phys., 10, 7085–7099, doi:10.5194/acp-10-7085-2010, 2010.

Jourdain, L., Worden, H., Worden, J., Bowman K., Q. Li, A. Eldering, S. Kulawik, G. Osterman, K. Boersma, and B. Fisher, Tropospheric vertical distribution of tropical Atlantic ozone observed by TES during the northern African biomass burning season, Geophys. Res. Lett., 34, L04810, doi:10.1029/2006GL028284, 2007.

Kanaya, Y., Komazaki, Y., Pochanart, P., Liu, Y., Akimoto, H., Gao, J., Wang, T., and Wang, Z.: Mass concentrations of black carbon measured by four instruments in the middle of Central East China in June 2006, Atmos. Chem. Phys., 8, 7637–7649, doi:10.5194/acp-8-7637-2008, 2008.

Kirchstetter, T. W., Novakov, T., Hobbs, P. V., and Magi, B.: Airborne measurements of carbonaceous aerosols in southern Africa during the dry biomass burning season, J. Geophys. Res, 108, 1783–1784, 2003.

Kondo, Y., Morino, Y., Takegawa, N., Koike, M., Kita, K., Miyazaki, Y., Sachse, G., Vay, S., Avery, M., and Flocke, F.: Impacts of biomass burning in Southeast Asia on ozone and reactive nitrogen over the western Pacific in spring, J. Geophys. Res, 109, D15S12, doi:10.1029/2003JD004203, 2004.

ACPD
12, 14363–14392, 2012

Kondo, Y., Matsui, H., Moteki, N., Sahu, L., Takegawa, N., Kajino, M., Zhao, Y., Cubison, M. J., Jimenez, J. L., Vay, S., Diskin, G. S., Anderson, B., Wisthaler, A., Mikoviny, T., Fuelberg, H. E., Blake, D. R., Huey, G., Weinheimer, A. J., Knapp, D. J., and Brune, W. H.: Emissions of black carbon, organic, and inorganic aerosols from biomass burning in North America and Asia in 2008, J. Geophys. Res.-Atmos., 116, D08204, doi:10.1029/2010jd015152, 2011.

Li, J., Wang, Z., Akimoto, H., Yamaji, K., Takigawa, M., Pochanart, P., Liu, Y., Tanimoto, H., and Kanaya, Y.: Near-ground ozone source attributions and outflow in central eastern China during MTX2006, Atmos. Chem. Phys., 8, 7335–7351, doi:10.5194/acp-8-7335-2008, 2008.

Maria, S. F., Russell, L. M., Turpin, B. J., Porcja, R. J., Campos, T. L., Weber, R. J., and Huebert, B. J.: Source signatures of carbon monoxide and organic functional groups in Asian Pacific Regional Aerosol Characterization Experiment (ACE-Asia) submicron aerosol types, J. Geophys. Res.-Atmos., 108, 8637, doi:10.1029/2003jd003703, 2003.

Pan, X. L., Kanaya, Y., Wang, Z. F., Liu, Y., Pochanart, P., Akimoto, H., Sun, Y. L., Dong, H. B., Li, J., Irie, H., and Takigawa, M.: Correlation of black carbon aerosol and carbon monoxide in the high-altitude environment of Mt. Huang in Eastern China, Atmos. Chem. Phys., 11, 9735–9747, doi:10.5194/acp-11-9735-2011, 2011.

Park, R. J., Jacob, D. J., Palmer, P. I., Clarke, A. D., Weber, R. J., Zondlo, M. A., Eisele, F. L., Bandy, A. R., Thornton, D. C., and Sachse, G. W.: Export efficiency of black carbon aerosol in continental outflow: Global implications, J. Geophys. Res., 110, 1–7, 2005.

Ram, K. and Sarin, M.: Spatio-temporal variability in atmospheric abundances of EC, OC and WSOC over Northern India, J. Aerosol Sci., 41, 88–98, 2010.

Rehman, I. H., Ahmed, T., Praveen, P. S., Kar, A., and Ramanathan, V.: Black carbon emissions from biomass and fossil fuels in rural India, Atmos. Chem. Phys., 11, 7289–7299, doi:10.5194/acp-11-7289-2011, 2011.

Reid, J. S., Hobbs, P. V., Liousse, C., Martins, J. V., Weiss, R. E., and Eck, T. F.: Comparisons of techniques for measuring shortwave absorption and black carbon content of aerosols from biomass burning in Brazil, J. Geophys. Res.-Atmos., 103, 32031–32040, 1998.

Reid, J. S., Koppmann, R., Eck, T. F., and Eleuterio, D. P.: A review of biomass burning emissions part II: intensive physical properties of biomass burning particles, Atmos. Chem. Phys., 5, 799–825, doi:10.5194/acp-5-799-2005, 2005.

Roden, C. A., Bond, T. C., Conway, S., and Pinel, A. B. O.: Emission factors and real-time optical properties of particles emitted from traditional wood burning cookstoves, Environ. Sci. Technol., 40, 6750–6757, 2006.

ACPD
12, 14363–14392, 2012

Shen, G., Yang, Y., Wang, W., Tao, S., Zhu, C., Min, Y., Xue, M., Ding, J., Wang, B., and Wang, R.: Emission factors of particulate matter and elemental carbon for crop residues and coals burned in typical household stoves in China, Environ. Sci. Technol., 44, 7157–7162, 2010.

Stier, P., Feichter, J., Kinne, S., Kloster, S., Vignati, E., Wilson, J., Ganzeveld, L., Tegen, I., Werner, M., Balkanski, Y., Schulz, M., Boucher, O., Minikin, A., and Petzold, A.: The aerosol-climate model ECHAM5-HAM, Atmos. Chem. Phys., 5, 1125–1156, doi:10.5194/acp-5-1125-2005, 2005.

Stohl, A., Hittenberger, M., and Wotawa, G.: Validation of the Lagrangian particle dispersion model FLEXPART against large-scale tracer experiment data, Atmos. Environ., 32, 4245–4264, 1998.

Streets, D., Yarber, K., Woo, J., and Carmichael, G.: Biomass burning in Asia: Annual and seasonal estimates and atmospheric emissions, Global Biogeochem. Cy., 17, 1099, doi:10.1029/2003GB002040, 2003.

Suthawaree, J., Kato, S., Okuzawa, K., Kanaya, Y., Pochanart, P., Akimoto, H., Wang, Z., and Kajii, Y.: Measurements of volatile organic compounds in the middle of Central East China during Mount Tai Experiment 2006 (MTX2006): observation of regional background and impact of biomass burning, Atmos. Chem. Phys., 10, 1269–1285, doi:10.5194/acp-10-1269-2010, 2010.

Tosca, M. G., Randerson, J. T., Zender, C. S., Flanner, M. G., and Rasch, P. J.: Do biomass burning aerosols intensify drought in equatorial Asia during El Niño?, Atmos. Chem. Phys., 10, 3515–3528, doi:10.5194/acp-10-3515-2010, 2010.

Vignati, E., Karl, M., Krol, M., Wilson, J., Stier, P., and Cavalli, F.: Sources of uncertainties in modelling black carbon at the global scale, Atmos. Chem. Phys., 10, 2595–2611, doi:10.5194/acp-10-2595-2010, 2010.

Yamaji, K., Li, J., Uno, I., Kanaya, Y., Irie, H., Takigawa, M., Komazaki, Y., Pochanart, P., Liu, Y., Tanimoto, H., Ohara, T., Yan, X., Wang, Z., and Akimoto, H.: Impact of open crop residual burning on air quality over Central Eastern China during the Mount Tai Experiment 2006 (MTX2006), Atmos. Chem. Phys., 10, 7353–7368, doi:10.5194/acp-10-7353-2010, 2010.

Yokelson, R. J., Urbanski, S. P., Atlas, E. L., Toohey, D. W., Alvarado, E. C., Crounse, J. D., Wennberg, P. O., Fisher, M. E., Wold, C. E., Campos, T. L., Adachi, K., Buseck, P. R., and Hao, W. M.: Emissions from forest fires near Mexico City, Atmos. Chem. Phys., 7, 5569–5584, doi:10.5194/acp-7-5569-2007, 2007.

ACPD
12, 14363–14392, 2012

Yu, H.: PHD thesis: Size distributions of elemental carbon, organic carbon, and polycyclic aromatic hydrocarbons in ambient aerosols of the Pearl River Delta region, 168 pp., Hong Kong University of Science and Technology, Hongkong, 2009.

ACPD
12, 14363–14392, 2012

Table 1. Description of the instrumentation at Mt Tai site.

Site & Period	Species	Instruments
Mt. Tai (2006 June) 36.26° N, 117.11° E 1534 m a.s.l	BC_e (PM_1) EC_a, OC (PM_1) CO CO_2	Multiple Angle Absorption Photometer (MAAP) Sunset ECOC analyzer with NIOSH temperature protocol non-dispersive infrared CO analyzer (Thermo Model 48C) NDIR Li-840 CO_2/H_20 Gas analyzer

ACPD
12, 14363–14392, 2012

Table 2. Detailed information on the biomass burning plumes measured at Mt. Tai.

Date	$EC_a(PM_1)$	$OC(PM_1)$	CO	$\Delta EC_a(PM_1)/\Delta CO$	$\Delta OC(PM_1)/\Delta CO$	$\Delta CO/\Delta CO_2$
	$\mu g\,m^{-3}$	$\mu g\,m^{-3}$	ppbv	$ng\,m^{-3}\,ppbv^{-1}$	$ng\,m^{-3}\,ppbv^{-1}$	$ppbv\,ppmv^{-1}$
7 Jun	8.8(4.5)	30.4(14.7)	1075.7(333.3)	12.9(0.9)	41.1(4.2)	40.6(5.9)
13 Jun	7.9(6.0)	29.1(18.1)	1021.6(340.0)	16.0(1.7)	51.2(4.4)	42.3(3.0)

ACPD
12, 14363–14392, 2012

Table 3. Statistical results for the dependence of OCRB carbonaceous aerosol correlations on transport time.

group	Transport time hours	$\Delta EC_a/\Delta CO$ ng m^{-3} ppbv^{-1}	$\Delta OC/\Delta CO$ ng m^{-3} ppbv^{-1}	$\Delta OC/\Delta EC_a$ –	$\Delta CO/\Delta CO_2$ ppbv ppmv^{-1}
1	10 ± 5.1	14.5 ± 2.2	47.5 ± 5.0	3.2 ± 0.2	45 ± 10.4
2	27.1 ± 24.8	13.5 ± 2.9	34 ± 11.3	2.4 ± 0.4	32.9 ± 7.4
3	32.7 ± 26.5	10.5 ± 1.4	29.6 ± 4.3	2.6 ± 0.3	38.6 ± 3.5

ACPD
12, 14363–14392, 2012

Table 4. Comparison of lifetime of black carbon aerosol from different studies.

Approach	Description	Lifetime (days)	Reference
GBAM	BC is hydrophobic when emitted and no subjective to wet deposition, then ages at an arbitrary rate of $7.1 \times 10^{-6}\ s^{-1}$ to a hydrophilic wet depositing form, which is removed in precipitation with the same efficiency as sulphate	6–10	Cooke and Wilson (1996)
TM5	BC is externally mixed and resides in the accumulation mode (mean: 0.14 µm)	4.7	Vignati et al. (2010)
TM5-M7	BC presents in insoluble and soluble Aitken modes and in the soluble accumulation/coarse modes by considering condensation of H_2SO_4 and coagulation.	6.2	
AGCM	A condensation and coagulation scheme An oxidative scheme A linear combination of condensation/coagulation and oxidative schemes	5.0 9.5 4.9	Croft et al. (2005)
ECHAM5-HAM	BC presents in insoluble and soluble Aitken modes and in the soluble accumulation/coarse modes	5.4	Stier et al. (2005)
Observation	Decay fitting with respect to transport time	4.3	This work

GBAM: global black carbon aerosol model
TM5: off-line global transport chemistry model using ECMWF ERA-40 meteorological data
M7: a microphysical aerosol model that allows the resolution of particle masses and numbers in seven internally mixed classes.
AGCM: Atmospheric general circulation model
ECHAM5: General Circulation Model. HAM: size-resolved aerosol model

ACPD
12, 14363–14392, 2012

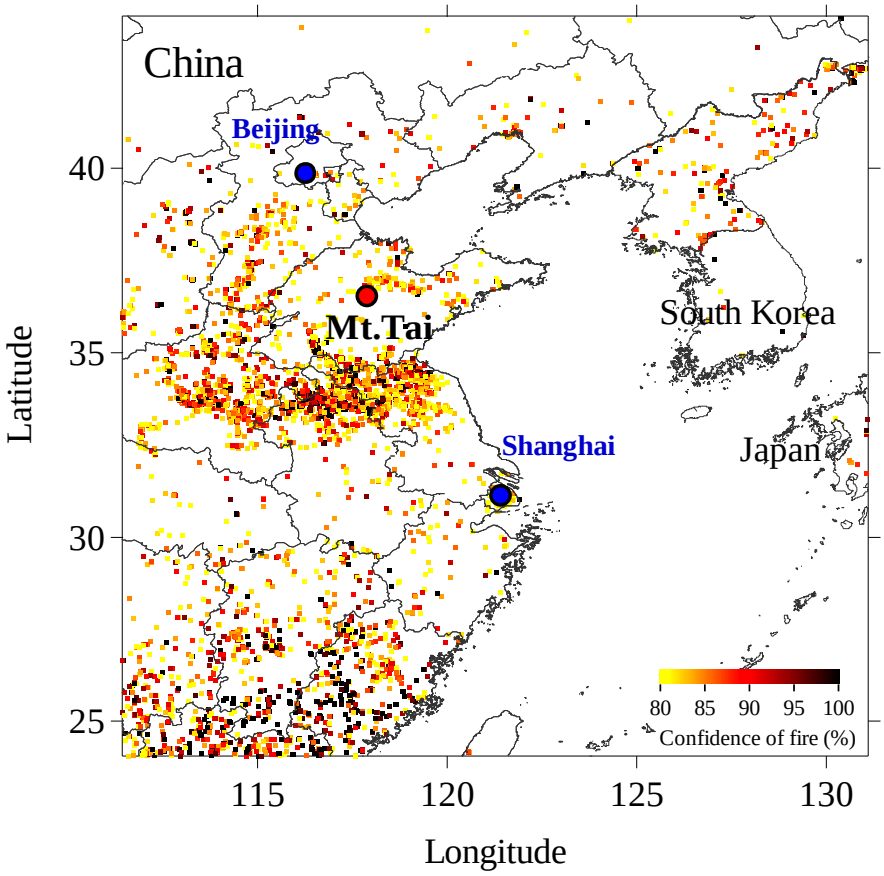

Fig. 1. Geographical location of the measurement site (Mt. Tai). The colored dots represent hotspots on June 2006 detected by a MODIS satellite. The colored shading indicates the confidence in the open biomass burning signals.

ACPD
12, 14363–14392, 2012

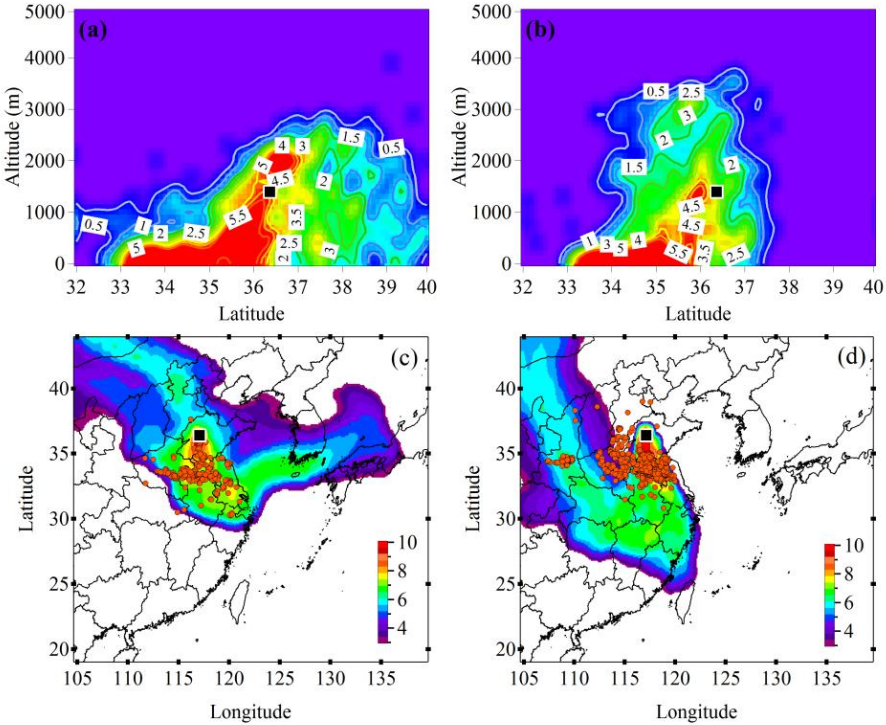

Fig. 2. Forward and backward simulations of convection movements of tracer particles using the FLEXPART_WRF model. The upper two panels show the vertical distributions (in the 117° E–118° E longitudinal band) of tracer concentrations during two OCRB episodes from forward simulations at 6 June, 23:00 LST **(a)** and at 12 June, 23:00 LST **(b)**. Footprint regions (<100 m in PBL) of aerosol samples at the summit of Mt. Tai from 6 June 18:00–7 June, 09:00 and 12 June, 18:00–13 June, 09:00 are shown in **(c)** and **(d)**, respectively. Colored shading indicates the natural logarithm of residence time (s) of tracers.

ACPD
12, 14363–14392, 2012

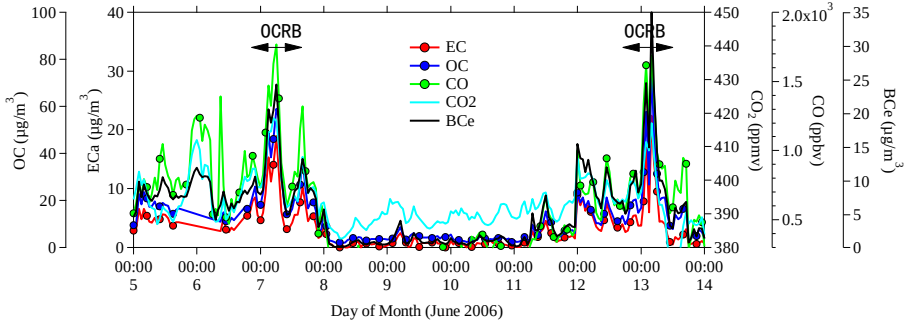

Fig. 3. Time series of carbonaceous aerosols, CO, and CO_2 concentrations measured at the summit of Mt. Tai.

ACPD
12, 14363–14392, 2012

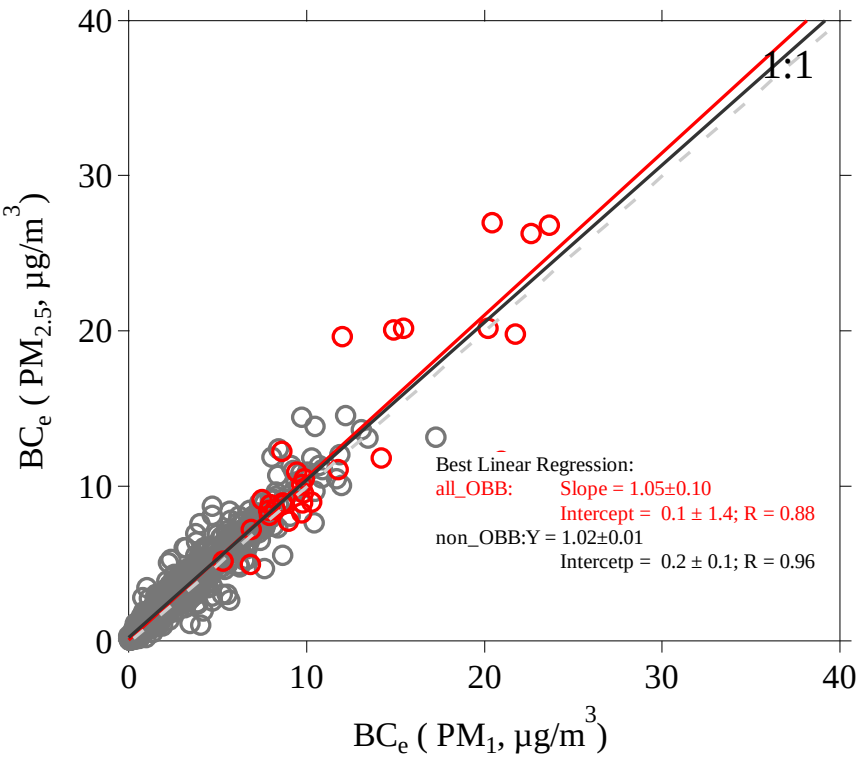

Fig. 4. Scatter plot of BC_e mass measured by MAAP with cutoffs of 1 μm and 2.5 μm. The gray dots indicate non-OCRB periods and red dots indicate OCRB-dominant episodes.

ACPD
12, 14363–14392, 2012

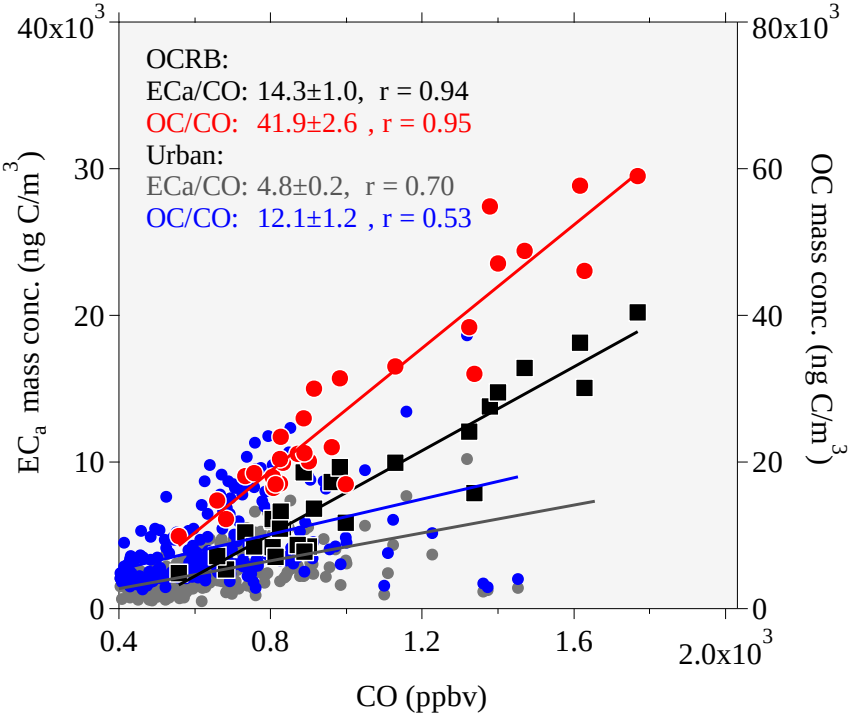

Fig. 5. Scatter plot and best linear fitting of EC_a-CO and OC-CO correlations for OCRB measured at Mt. Tai.

ACPD
12, 14363–14392, 2012

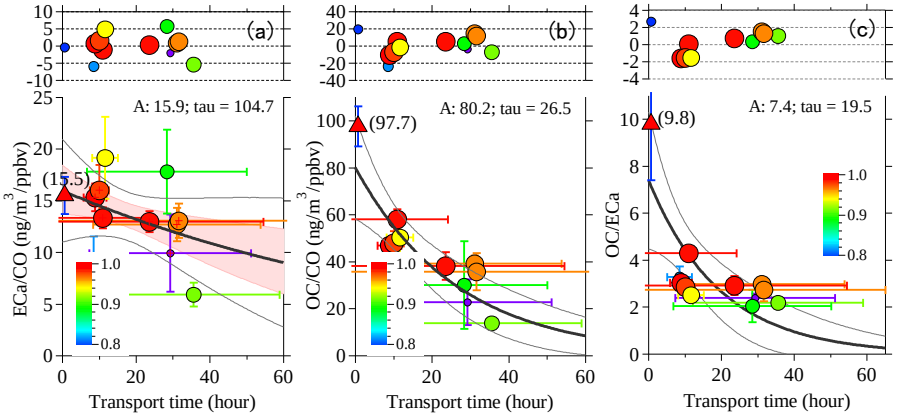

Fig. 6. Variations in EC_a-CO **(a)**, OC-CO **(b)** and OC-EC_a **(c)** correlations with transport time and residuals of fittings. Solid triangles indicate measurements at Rudong. Solid circles represent the statistical results from 6 June, 10:00 LST–7 June, 09:00 LST and from 12 June, 18:00 LST–13 June, 09:00 LST at the summit of Mt. Tai. The correlation coefficients for each time window are indicated by colored shading in the plot. Confidence bands at the 95 % confidence interval are shown as gray lines in the figure. The pink band in **(a)** is the confident band for the fitting for the data which ECa-CO correlation efficient are greater than 0.95.

ACPD
12, 14363–14392, 2012

Estimation of lifetime of carbonaceous aerosol

X. L. Pan et al.